

CCA-1509

YU ISSN 0011-1643

UDC 541

Original Scientific Paper

»Common Denominators« by the MOV B Method: The Structures of H₂O, H₂O₂, and Their Derivatives

Nicolaos D. Epiotis*, James R. Larson, and Hugh H. Eaton

Contribution from the Department of Chemistry, University of Washington, Seattle, Washington 98195, U.S.A.

Received 17, October 1983

We present a detailed illustration of how qualitative MOV B theory can be applied to problems of molecular stereochemistry at different levels of sophistication by using H₂O, H₂O₂, and their derivatives as target systems. Two problems long thought to be unrelated, the geometries of H₂O and H₂O₂, are shown to be identical, to a first approximation.

INTRODUCTION

Many years after the experimental demonstration that H₂O has a bent¹ and H₂O₂ a gauche² geometry, the reason behind these stereochemical preferences still remain obscure. One of the simplest species of the AH_{*n*} (*n* = 2, 3, 4, 5, and 6) family, H₂O has been the target of many theoretical investigations aimed at unraveling the electronic factors which dictate the preferred geometry of AH_{*n*} molecules. Nonetheless, despite many years of extensive research, questions remain. This state of affairs is reflected in old as well as recent publications offering different views as to why H₂O is bent,³⁻⁶ why H₂S is more bent than H₂O,⁶⁻⁸ what constitutes a lone pair in H₂O and AH_{*n*} molecules,⁹ and so on. The situation is not different in the case of H₂O₂, one of the simplest illustrators of conformational isomerism. Once again, despite many efforts, a consensus has not yet been reached as to why H₂O₂ adopts a gauche conformation,¹⁰⁻¹³ why the dihedral angle decreases as one makes a transition from H₂O₂ (120°) to H₂S₂ (90.5°),¹⁴ etc., although it must be said that the hyperconjugation model affords an appealingly simple rationalization of some of these trends.¹¹⁻¹³ In this work, we use the MOV B theory of ground molecular structure^{15,16} in order to demonstrate that the lowest energy structures of H₂O, H₂O₂ and their derivatives are determined by the same electronic factor. By pointing out the common denominator in these two apparently unrelated problems, we hope to demonstrate the capability of MOV B theory to act as a »bridge-builder« across different areas of research in chemistry and physics, a theme which we will pursue further in following publications. In addition, we use MOV B theory in order to analyze the effect of ligand lone pairs on molecular stereochemistry in a way which reveals the new horizons which are opened by this theoretical formalism.

This paper is essentially divided into two parts. In the first part, we examine the stereochemistry of AX₂ and A₂X₂ molecules (A = O and S) by

treating X as a univalent ligand and neglecting the presence of any additional lone pairs. In the second part, we examine the influence of ligand lone pairs on different properties of OX_2 and O_2X_2 and we show that the indirect effect of these lone pairs can be completely understood only at the level of poly-determinantal MO theory, the equivalent of MOVb theory. Throughout the paper, a conscious effort is made to interrelate different theoretical formalisms and point out common denominators and differences. Thus, it is important that the reader be aware of the equivalence relationships of different MO and MOVb theoretical methods.¹⁵ These are spelled out in Table I. HMO, EHMO, and SCF-MO theories are collectively referred to as Single Determinant (SD) MO theory. They all fail to describe adequately interelectronic repulsion because of the approximations employed. These are indicated in Table I.

TABLE I

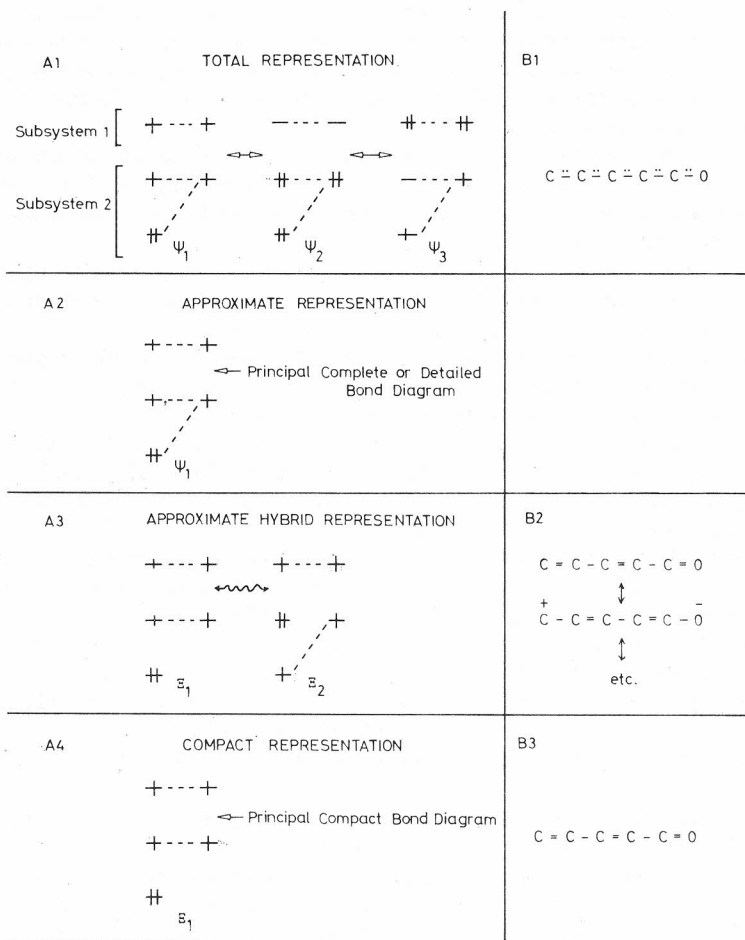
Approximate and Rigorous Types of Valence Bond and Molecular Orbital Theories^a

VB — Type Theory	MO — Type Theory	Approximation
VB HL (delocalized AO's) MOVb	SCF — MO — CI	None
HL (localized AO's)	—	Truncation
—	3 × 3 SCF — MO — CI	Truncation
—	SCF — MO	Constraint
NDO — VB NDO — MOVb	—	Integral
	NDO — SCF — MO	Integral and Constraint
EHVB (S ≠ O) EHMOVb (S ≠ O)	EHMO (S ≠ O)	Integral and Constraint
HVB (S = O) HMOVb (S = O)	HMO (S = O)	Integral and Constraint

^a Theories within a row are equivalent. HL stands for Heitler-London and S is the AO overlap integral.

THEORETICAL BACKGROUND

The bond diagrammatic representation of molecules is the foundation of MOVb theory. To a certain extent, this kind of representation is analogous to the one on which »resonance theory« is based and this fact can be projected by a comparison of the various ways in which MOVb theory depicts a *ground state* species made up of three core and two ligand MO's which define two subsystems containing a total of six electrons (6/5 species) and the ways in which »resonance theory« depicts a *ground state* six-electron-six-AO (6/6 species) such as the pi system of $CH_2=CH-CH=CH-CH=O$. The different pictorial representations are shown in Scheme 1 so that the analogies are made evident. First of all, the *total* MOVb diagrammatic representation of the 6/5



Scheme 1

species is obtained by a linear combination of three *complete* bond diagrams, as in A1, which describe the optimal linear combination of *all* MOVB Configuration Wavefunctions (CW's). By the same token, a *total* VB diagrammatic representation of the 6/6 species can be obtained by writing a »dot structure«, as in B1, and taking this to mean the optimal linear combination of all VB CW's. Next, we can approximate the MOVB wavefunction of the 6/5 species by one *complete* (or *detailed*) bond diagram (A2). No simple VB representation analogy can be given in this case. Alternatively, we can approximate the MOVB wavefunction by a linear combination of *compact* bond diagrams, as in A3, in the way described before. These compact bond diagrams have common CW's and they also exclude a set of extrinsic CW's which must necessarily be added in quantitative as well as in some qualitative applications of MOVB theory. The VB analogue in this case is the hybrid representation of the 6/6 species by a set of »important« VB CW's, as in B2. Finally, we can obtain a

compact representation of the 6/5 species by simply eliminating all compact bond diagrams except the one containing the dominant CW or CW's, as in A4. Correspondingly, we can obtain a compact representation of the 6/6 species by eliminating all but the CW which makes the major contribution to the VB resonance hybrid, as in B3.

With this introduction, let us now take a close look at the actual procedure by which one can *explicitly* calculate the electronic states of a molecule so that a pictorial (bond diagrammatic) representation thereof becomes feasible. The necessary steps are the following:

(a) The molecule is subdivided into two (or more) fragments and the (atomic or molecular) orbitals of each fragment are computed and classified according to *local* symmetry in a point group theoretical sense.

(b) All fragment orbitals which belong to one irreducible representation (Γ_a) of the subgroup of the composite system (the molecule) dictated by *local* symmetry are said to define a subsystem denoted by Ω_a .

(c) A particular distribution of the electrons within the various subsystems is said to define an MOV B Tableau denoted by T_i . Each T_i can be ascribed physical meaning to the extent that it features a unique set of multi-center bonds linking the two fragments.

(d) Each MOV B Tableau is associated with a set of MOV B Configuration Wavefunctions (CW's) generated by permuting the electrons among the fragment orbitals. The set is denoted by U_i and the CW's by Φ_m .

e) By using a variational or perturbational procedure one constructs the zero order states corresponding to each T_i in either of two ways:

1) By departing from the U_i set of CW's corresponding to T_i . The resulting zero order states are denoted by $\Psi_{ij}(D)$ where i is a tableau or set and j a state index. Each $\Psi_{ij}(D)$ can be represented pictorially by a *detailed bond diagram*.

2) By departing from the U_i set of CW's corresponding to T_i and partitioning into V_k subsets which may or may not intersect. By »intersecting« we mean that two such subsets have one or more common CW's. The partitioning is entirely arbitrary and depends on chemical intuition. Each V_k subset can be used to generate zero order substates denoted by Ξ_{kl} where k is a subset and l a substate index. A given subset may contain only one element, *i. e.*, one CW, in which case $\Xi_{k0} = \Phi_m$. Each Ξ_{kl} generated by a subset V_k which contains appropriate element can be represented by a *compact bond diagram*. Replacing now the U_i basis of Φ_m 's by the W_i basis of Ξ_{kl} 's we can once again compute the zero order states now denoted by $\Psi_{ij}(R)$. In all applications of MOV B theory we use the convention of choosing the V_k 's so that the resulting Ξ_{k0} has a maximum number of interfragmental bonds. The way in which individual CW's taken in aggregate define bonds has been discussed in the original work.

(f) Starting with the Ψ_{ij} 's, one can finally compute the rigorous electronic states, Θ_n 's.

(g) For the choice of V_k 's specified above and by switching to a simpler indexing system, we can write:

$$\Psi_{i0}(R) \approx \sum_k c_{k0} \Xi_{k0} = \sum_q c_q \Xi_q \quad (j = 0)$$

$$\Psi_{i1}(R) \approx \sum_k c_{k1} \Xi_{k1} = \sum_r c_r \Xi_r \quad (j = 1)$$

and

$$\Theta_n = \sum_i \sum_j c_{ij} \Psi_{ij} = \sum_n c_n \Psi_n$$

In most qualitative applications we can truncate the expansions of $\Psi(R)$ and Θ_n to the one or two most important terms:

$$\Psi_\mu(R) \approx c_1 \Xi_1 + c_2 \Xi_2$$

and

$$\Theta_n \approx c_1 \Psi_1 + c_2 \Psi_2$$

Note that a lower j index does not necessarily imply a lower energy Θ_n . For example, the first excited state Θ_1 may have a principal contributor Ψ_{x1} while the higher lying Θ_2 has a principal contributor Ψ_{y0} .

The overall approach can be best understood by means of a specific example and to this extent we have included in an Appendix the construction of the electronic states of the carbon-carbon double bond of ethylene.

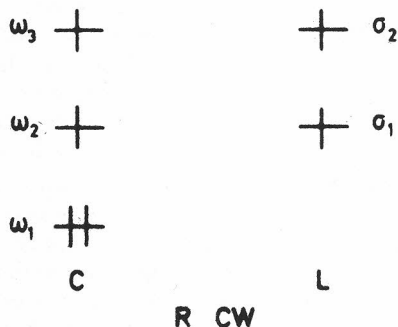
We now restrict our attention to ground state stereochemistry and we outline a simple recipe for approximating Θ_0 of a given geometry. This can be used in a routine manner by the practicing chemist who has little knowledge of quantum mechanics:

a) A molecule or complex is divided into a core fragment (C) and a fragment which contains all ligands (L).

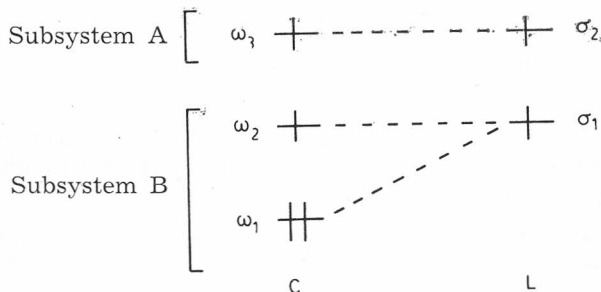
(b) The *principal detailed bond diagram*, Ψ_1 , is constructed for every assumed geometry of the molecule or complex by following these steps:

1) The core and ligand symmetry adapted orbitals are generated either from first principles or by explicit computation.

2) The electrons are arranged in the core and ligand orbitals in a way which generates the reference, »perfect pairing« (R) CW subject to the symmetry constraints imposed by the geometry in question. This is the open shell CW which places core and ligand electron pairs in the lowest energy orbitals of core and ligand subject to the requirement that it generates the *maximum* number of core-ligand bonds through spin pairing. For example, the R CW of a six-electron-five-orbital system where the lowest two core (ω_1 and ω_2) and the lowest ligand (σ_1) orbitals are of one symmetry type and the highest core (ω_3) and ligand (σ_2) orbitals are of a different symmetry type is written as follows:



3) The detailed bond diagram for the geometry in question is constructed by adding dashed lines to the drawing of the R CW in order to denote all possible CW's which can be generated by the implied electron shifts under the imposed symmetry constraints. For example, the detailed bond diagram corresponding to the previous case becomes:



Detailed Bond Diagram

(c) Starting from the principal detailed bond diagram, *i. e.*, the $\Psi_1(D)$ representation, one can develop the $\Psi_1(R)$ representation by writing the two or three most important Ξ_q 's.

(d) By examining either $\Psi_1(D)$, $\Psi_1(R)$ or Ξ_1 , we may determine the type of bonding imposed by core and ligand orbital symmetry in each case recalling that there are three bonding »flavors«: D bonding which permits electrons to descend to low lying orbitals, U bonding which confines some of the electrons to high lying orbitals, and H bonding which represents a hybrid of D and U bonding accompanied by impairment of core-ligand spatial overlap, at least in most cases of interest. Loss of spatial overlap is indicated by affixing a dagger superscript to the appropriate letter, most often H. The letter (U, H[†], and D) assignment is always made in a relative sense and the selection rules are: D is always better than H[†] and U bonding but H[†] may be superior or inferior to U bonding depending on whether deexcitation is more important than loss of spatial overlap or *vice versa*. It should be emphasized that the pairwise assignment of the letters U, H[†], and D describes the difference in bonding of two isomeric forms *expressed* by the corresponding $\Psi_1(D)$ and $\Psi_1(R)$ representations or *implied* by the principal compact bond diagrams, Ξ_q 's. Each detailed bond diagram is a pictorial approximate representation of the optimal MOVb wavefunction of the system in question. In addition, it shows explicitly the number and types of independent »many electron-many center« bonds which join the core and the ligand fragments. For the reader's convenience, the symmetry of each orbital is specified either by the formal point group label or by the letters S (symmetric) and A (antisymmetric) which define the behavior of the orbital upon performance of an obvious symmetry operation (*e. g.*, rotation about an axis, reflection through a plane, *etc.*).

In dealing with detailed bond diagrams, it must be kept in mind that, because of the way in which the R CW is defined and the way in which the detailed bond diagram is constructed, neither the »parent« R CW is *necessarily* the lowest energy CW nor the principal compact bond diagram (Ξ_1 in Scheme 1) is *necessarily* the one directly reflected by the detailed bond diagram *as written*, although in most problems of interest this is indeed the case. However, neither

of these semantic difficulties is an obstacle to the qualitative application of MOVB theory. Consistent with the above stated philosophy, we assign *formal charge* to C and L by reference to the perfect pairing CW projected by the bond diagram as written. Thus, for example, we have written C and L underneath the bond diagram shown above because we assumed that neutral C has four electrons and neutral L two electrons. Had neutral C had three and neutral L also three electrons, we would have written C⁻ and L⁺ underneath the bond diagram, keeping always in mind that these are formal charges with the real ones being determined by all CW's which make up the MOVB wavefunction.

RESULTS AND DISCUSSION

The Structures of H₂O and its Derivatives

Water can be viewed as a composite of O and H₂. The basis fragment orbitals are the valence AO's of O and the symmetry adapted valence MO's of H₂. The CW's required for the description of Linear (L) and Bent (B) H₂O are constructed by permuting all eight valence electrons among the various fragment valence orbitals. The $\Psi_1(D)$ representations are shown in Figure 1 and

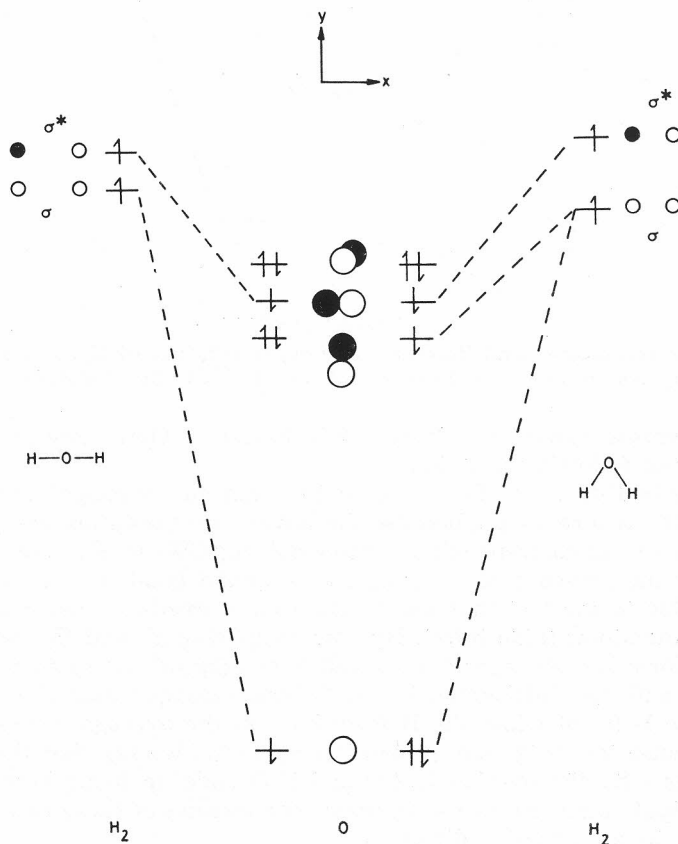


Figure 1. Detailed MOVB bond diagrams for linear and bent H₂O.

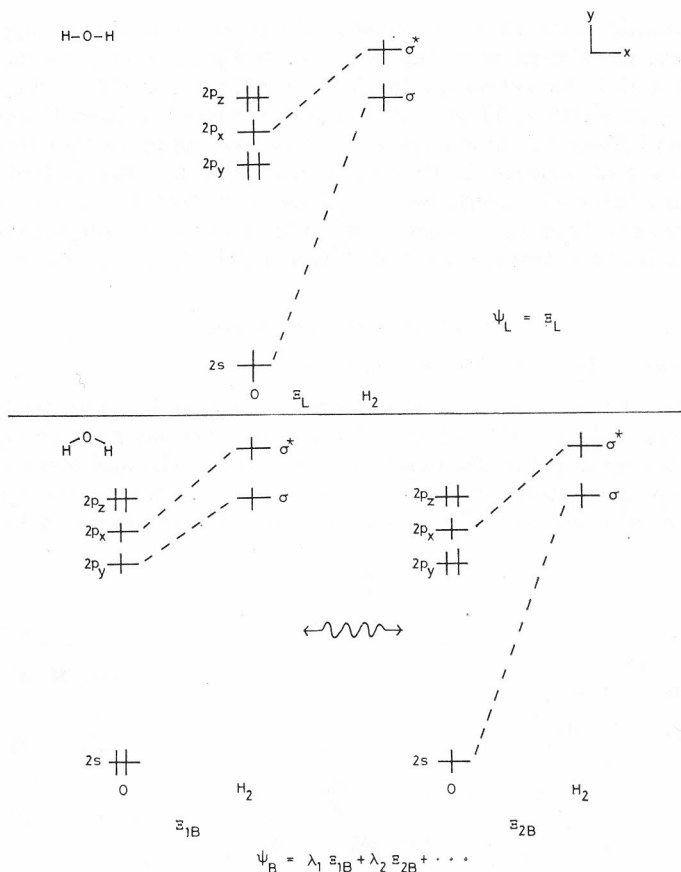


Figure 2. The resonance bond diagrammatic representation of linear and bent H_2O . Wiggly double arrows indicated that the two ϵ_i 's have common CW's.

the $\Psi_1(R)$ representations are displayed in Figure 2. These now provide direct answers to the following questions:

(a) Why is H_2O bent? First, we realize that the principal compact bond diagram of the B form is ϵ_{1B} because the lower core excitation energy (defined with respect to the corresponding perfect pairing CW) in ϵ_{1B} more than compensates for the presence of a stronger core-ligand bond in ϵ_{2B} ($2s-\sigma$ stronger than $2p-\sigma$) due to the fact that the $2s$ has greater *overlap binding ability* than $2p$ in first row atoms (*vide infra*). By now comparing ϵ_L and ϵ_{1B} , we recognize that the L form has stronger core-ligand bonds ($2p_x-\sigma^*$ interaction stronger in the L form and $2s-\sigma$ interaction in the L form stronger than the $2p_y-\sigma$ interaction in the B form) while the B form has, on the average, lower excitation energy. Because the $2s-2p$ energy gap is very large, we say that the excitation factor »beats out« the overlap factor and H_2O ends up being bent. In saying so, we anticipate other molecules in which the conflict of these two effects will be resolved in an opposite direction.

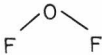
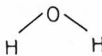
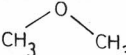
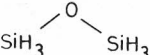
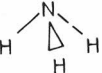

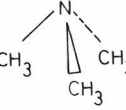
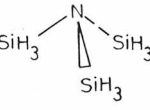
(b) What are the stereochemical consequences of replacing H by sigma acceptor, *i. e.*, more electronegative, ligands, X? The oxygen core is a better

donor in \mathcal{E}_{1B} than in \mathcal{E}_{2B} . Hence, replacement of H by X will increase the λ_1/λ_2 ratio because the lowest energy CW which has two electrons transferred from core to ligand belongs only to \mathcal{E}_{1B} . This, in turn, will increase the $2p$ character of the orbitals of O which are directed towards the ligands since the two core-ligand bonds described by \mathcal{E}_{1B} involve exclusive participation of the oxygen $2p$ AO's. As a result, the angle of H₂O will »shrink«. Exactly the opposite will occur when X is more electropositive than H.

This analysis is compatible with many known facts. Thus, the vibrational structure of the photoelectron spectrum of H₂O suggests that the oxygen lone pair has predominant s character.¹⁷ Experimental data pertaining to the effect of ligand electronegativity on the shapes of OX₂ and NX₃ molecules have been repeatedly summarized and/or discussed in papers and monographs.¹⁸ Some results which appear to be in excellent agreement with the MOVb model are given in Table II.¹⁹⁻²⁰

(c) What are the stereochemical consequences of replacing O by S? At first sight, it appears that this will also increase the λ_1/λ_2 ratio and cause angle

TABLE II
Electronegativity Dependence of Angles in OH₂ and NX₃ Molecules

Molecule	\angle XOX	X Electronegativity*	Ref.
	103°	3.98	19a
	105°	2.10	19b
	112°	2.55	19c
	144°	1.90	19d
	107°	2.10	20a
	102°	3.98	20b
	111°	2.55	20c
	120°	1.90	20d

* The electronegativity of X is equated to the electronegativity of the atom of X directly attached to the central atom.

»shrinkage« for the reasons explained in (b). However, more than that is actually involved and this is indicated by the fact that the angle »shrinkage« of H_2S^{21} is much more dramatic than the angle shrinkage in F_2O or the angle opening in $(\text{CH}_3)_2\text{O}$ (always relative to H_2O). Indeed, the reasons behind the stereochemical difference between water and hydrogen sulfide have been actively debated⁶⁻⁸ and, thus, this topic deserves a more detailed discussion. However, before we proceed any further, we digress in order to consider differing electronic features of first and second row atoms which have not yet been fully appreciated. The problem can be brought to focus by a specific comparison of H—F and H—Cl where we inquire about the relative magnitudes of the following matrix elements:

$$(a) \langle 1s_{\text{H}} | \hat{O}' | 2s_{\text{F}} \rangle \text{ versus } \langle 1s_{\text{H}} | \hat{O}' | 2p_{\text{F}} \rangle$$

$$(b) \langle 1s_{\text{H}} | \hat{O}' | 3s_{\text{Cl}} \rangle \text{ versus } \langle 1s_{\text{H}} | \hat{O}' | 3p_{\text{Cl}} \rangle$$

We define the following quantities:

$$\Delta h_{\text{F}} = \langle 1s_{\text{H}} | \hat{O}' | 2p_{\text{F}} \rangle - \langle 1s_{\text{H}} | \hat{O}' | 2s_{\text{F}} \rangle \quad (1)$$

$$\Delta h_{\text{Cl}} = \langle 1s_{\text{H}} | \hat{O}' | 3p_{\text{Cl}} \rangle - \langle 1s_{\text{H}} | \hat{O}' | 3s_{\text{Cl}} \rangle \quad (2)$$

Each mono-electronic matrix element can be evaluated by using the Wolfsberg-Helmholz approximation.²²

$$h_{tu} = \langle t | \hat{O}' | u \rangle = K (h_t + h_u) s_{tu} / 2 \quad (3)$$

where t and u are AO's, h_t the one-electron energy of t , s_{tu} the overlap integral of t and u and $1.4 < K < 2.0$.

The results given in Table III reveal two very important trends:

TABLE III
*s versus p Overlap Bonding Abilities of First and Second Row Atoms**

AO Resonance Integral	$-h/K$ eV	$\Delta h/K$ eV
$\langle 1s_{\text{H}} \hat{O}' 2s_{\text{F}} \rangle$	23.29	11.78
$\langle 1s_{\text{H}} \hat{O}' 2p_{\text{F}} \rangle$	11.51	
$\langle 1s_{\text{H}} \hat{O}' 3s_{\text{Cl}} \rangle$	16.78	3.47
$\langle 1s_{\text{H}} \hat{O}' 3p_{\text{Cl}} \rangle$	13.31	
$\langle 1s_{\text{H}} \hat{O}' 2s_{\text{O}} \rangle$	23.82	12.00
$\langle 1s_{\text{H}} \hat{O}' 2p_{\text{O}} \rangle$	11.82	
$\langle 1s_{\text{H}} \hat{O}' 2s_{\text{S}} \rangle$	15.16	2.35
$\langle 1s_{\text{H}} \hat{O}' 2p_{\text{S}} \rangle$	12.81	

* Calculated using H—X distances appropriate to H—F, H—Cl, H_2O , and H_2S .

(a) A first row atom binds much more strongly with the 2s than with the 2p AO.

(b) A second row atom again binds more strongly with the 2s AO but the differential binding ability of the 3s and 3p AO's is nowhere as large as that of first row atoms.²³

We emphasize that by the term »binding ability« we refer to the »overlap binding ability« of the atom. For the purpose of simplifying the analysis, we can say that the following two relationships hold:

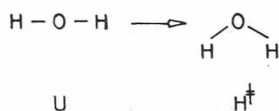
$$\Delta h_X \gg 0$$

$$\Delta h_Y \approx 0$$

where X = F, O, N, C and Y = Cl, S, P, Si.

It follows then that the reason why the angle of H₂S (92°)²¹ is 13° smaller than that of H₂O (105°) is mainly due to the fact that replacement of O by S increases λ_1/λ_2 not only because S is more electropositive than O but also because S binds equally well with its 3s and 3p AO's while O binds much better with its 2s rather than its 2p AO.^{24,25} A second factor which probably operates in a way that causes H₂S to have a smaller angle than H₂O is indeed nonbonded overlap repulsion, as pointed out by Hall.^{6a} Exactly how this type of repulsion arises is made obvious by casual inspection of the $\bar{\epsilon}_{1B}$ and focusing attention on the corresponding perfect pairing CW. As the HOH angle decreases and the two hydrogens approach each other, the unsymmetrical splitting of σ and σ^* raises the energy of the R CW and, hence, the energy of the entire system. In H₂S with HSH equal to the equilibrium angle of H₂O the longer bonds become responsible for a larger H--H nonbonded distance and smaller overlap repulsion. As a result, the HSH angle can shrink further before assuming a value at which the H--H overlap nonbonded overlap repulsion in H₂S is as severe as that in H₂O.

The discussion of the stereochemistry of H₂O and its derivatives makes plain that stereochemical predictions can be made in many cases by mere inspection of the principal compact bond diagrams appropriate to different geometries. Indeed, by simply writing down the $\bar{\epsilon}_1$'s of L and B water, extracted from the corresponding Ψ_1 (D) or Ψ_1 (R), we could deduce that the higher symmetry L form constitutes a U and the lower symmetry B form an H[‡] geometry. Accordingly, the L → B transformation can be symbolized as follows:



The process is exothermic because electron demotion more than compensates for bond weakening accompanying the U → H[‡] conversion because the 2s — 2p energy gap of O is very large.

The Structures of H₂O₂ and its Derivatives

The detailed bond diagrams of trans (T) and gauche (G) H₂O₂ are shown in Figure 3 and the corresponding principal compact diagrams in Figure 4. It is immediately obvious that the higher symmetry T form corresponds to a U-

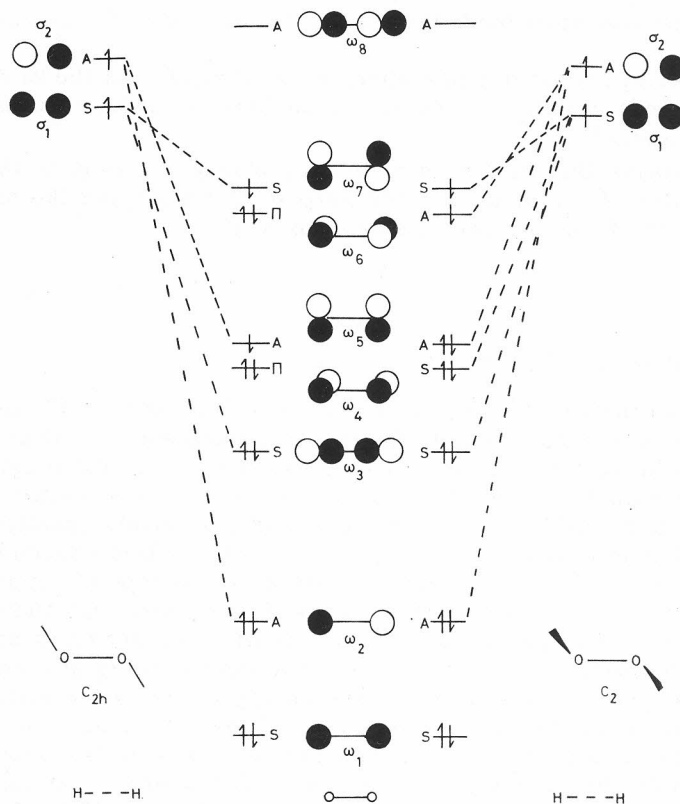
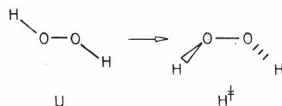


Figure 3. Detailed MOVB bond diagrams for trans and gauche H_2O_2 .

bound system and the lower symmetry G form to an H^\ddagger -bound system. Accordingly, the $\text{T} \rightarrow \text{G}$ transformation can be symbolized as follows:



The trans U form is $\omega_5 \rightarrow \omega_7 (\pi \rightarrow \pi^*)$ excited relative to the gauche H^\ddagger form and the corresponding excitation energy is appreciably large. Thus, in the $\text{T} \rightarrow \text{G}$ conversion, deexcitation is expected to overbalance loss of spatial overlap. As a result, the G conformer is expected to have lower energy than the T conformer. *This analysis makes evident the fact that the $\text{L} \rightarrow \text{B}$ transformation of H_2O and the $\text{T} \rightarrow \text{G}$ transformation of H_2O_2 are directly related problems, as they are both driven by $\text{U} \rightarrow \text{H}^\ddagger$ conversions.* Accordingly, the effect of structural modification on the dihedral angle of A_2X_2 must be identical to the effect of the same modification on the planar angle of AX_2 . Before we consider the actual experimental results, we open a parenthesis in order to define some operationally useful experimental observables.

The angle of linear AX_2 is 180° and the angle of bent AX_2 can be denoted by x . Then, $x' = 180^\circ - x$ represents a measure of the deviation of AX_2 from a pure U-bound system. Similarly, the dihedral angle of planar A_2X_2 can be 0°

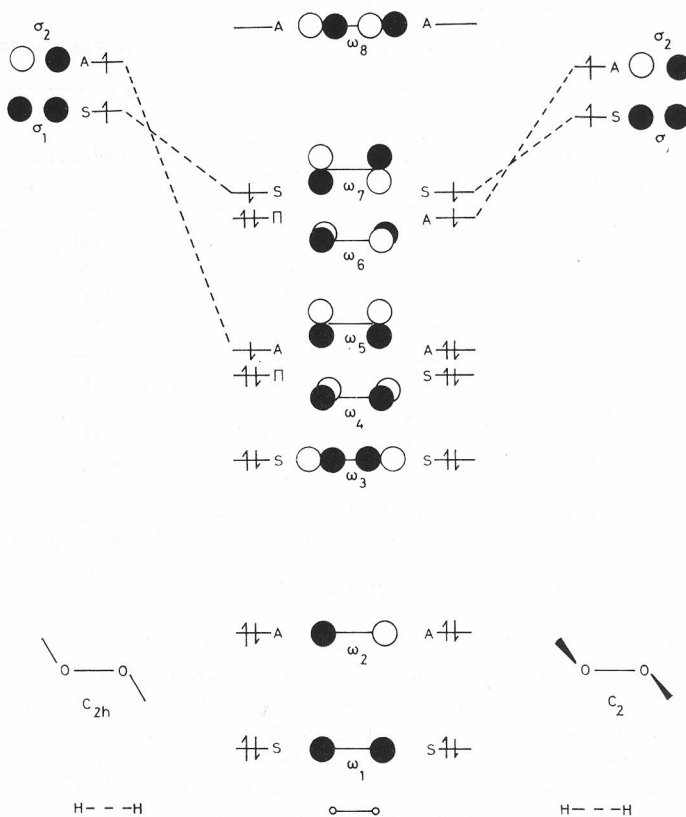


Figure 4. Principal compact MOVB diagrams for trans and gauche H₂O₂.

(cis) or 180° (trans) and the dihedral angle of nonplanar A₂X₂ can be denoted by ϕ . Now, it can be easily shown through construction of bond diagrams that, though the cis and trans planar forms of A₂X₂ involve different type of bonding, as ordained by orbital symmetry, they *both* are U species relative to the H[±] gauche form. Accordingly, if $\phi' = |180^\circ \text{ (or } 0^\circ) - \phi|$, the maximal deviation of A₂X₂ from a pure U-bound system will occur for $\phi = 90^\circ$.

With the above definitions in mind, the data presented in Table IV make unambiguously clear that structural modification effects operate analogously in AX₂ and A₂X₂ systems. Specifically, we note the following:

(a) As H is replaced by F in OH₂ and O₂H₂, *i. e.*, as ligand electronegativity increases, x' increases and ϕ' tends towards the limiting value of 90°.

(b) As O is replaced by S in OH₂ and O₂H₂, *i. e.*, as core electropositivity increases and the differential overlap binding abilities of the *s* and *p* AO's in XH₂ (X = O, S) and those of the $\omega_2 - \omega_7$ MO's in X₂H₂ (X = O, S) change, the same trends are manifested as in (a).

(c) As the ligand is varied from F to Cl to Br to I, *i. e.*, as electronegativity decreases within a set of ligands which belong to one column of the Periodic Table, x' steadily decreases and ϕ' increasingly deviates from the limiting value of 90°. The trend is exactly opposite to that in (a).

TABLE IV
The Bond Angles of Prototypical X_2O_2 , X_2O and X_3N Molecules^a

Molecule	$\overset{\wedge}{\text{XAAX}}$ Dihedral Angle	Molecule	$\overset{\wedge}{\text{XAX}}$ Angle	Molecule	$\overset{\wedge}{\text{XAX}}$ Angle
H_2O_2	120°	H_2O	104°	NH_3	107°
F_2O_2	88°	F_2O	103°	NF_3	102°
Cl_2O_2	—	Cl_2O	111°	NCl_3	108°
Br_2O_2	—	Br_2O	—	NBr_3	—
H_2S_2	91°	H_2S	92°	PH_3	93°
F_2S_2	88°	F_2S	98°	PF_3	97°
Cl_2S_2	85°	Cl_2S	103°	PCl_3	100°
Br_2S_2	83° ^b	Br_2S	—	PBr_3	—

^a Numerical Data and Functional Relationships in Science and Technology, New Services, Group II, Vol. 7 Landolt-Börnstein, Springer-Verlag: New York and Berlin, 1976.

^b E. Hirota, *Bull. Chem. Soc. Jpn.* **31** (1958) 130.

(d) Some apparently »abnormal« trends, which could not be easily rationalized before, now make very good sense. For example, replacement of H by F in OH_2 shrinks the angle but the same replacement in SH_2 opens the angle. This is due to the fact that the relative weights of the \mathcal{E}_{1B} and \mathcal{E}_{2B} resonance bond diagrams are different in H_2O and H_2S . In the former case, they are comparable, while, in the latter case, they are very different with that of \mathcal{E}_{1B} far exceeding that of \mathcal{E}_{2B} . Accordingly, H_2O will rehybridize upon substitution of H by F so that \mathcal{E}_{1B} becomes relatively more important than \mathcal{E}_{2B} . By contrast, H_2S cannot do so since \mathcal{E}_{1B} is already the dominant contributor, or, in other words, H_2S is essentially D^{\pm} -bound for reasons explained above. Accordingly, replacement of H by F can only introduce nonbonded repulsion which ultimately causes an opening of the angle.²⁶

Bond Lengths

What does MOVb theory predict with regards to the bond lengths changes which accompany the transformation of L to B H_2O and T to G H_2O_2 ? Inspection of the bond diagrams shown in Figures 1 and 3 leads to the following conclusions:

(a) In L H_2O , one multicenter bond is made by utilization of the $2p_x$ and the other by utilization of the $2s$ AO of O. By contrast, in B H_2O , one multicenter bond is made again by utilization of the $2p_x$ AO of O but the other is now made by hybridization of the $2p_y$ and $2s$ O AO's. Since the $2s$ AO binds more strongly than the $2p$ AO and since s character is lost upon $L \rightarrow B$ transformation, we conclude that the O—H bonds will be longer in the B than in the L form. For the same reasons, the N—H bonds will be shorter in planar than in pyramidal NH_3 .

(b) Similarly, in T H₂O₂ one multicenter bond is made by hybridization of the ω_2, ω_5 MO's and the other by the hybridization of the ω_3, ω_7 MO's of the O₂ fragment. By contrast, in G H₂O₂, one multicenter bond is made by hybridization of the $\omega_2, \omega_5, \omega_6$ MO's but the other is now made by the hybridization of the $\omega_3, \omega_4, \omega_7$ MO's of O₂. Examination of the nature of these various MO's reveal that *s* character is lost upon T → G transformation. Hence, the O—H bonds are predicted to be longer in G than in T H₂O₂.

(c) The T → G transformation in H₂O₂ is accompanied by core deexcitation which depopulates an antibonding MO, ω_6 , and populates a bonding MO, ω_5 . Hence, the O—O bond is predicted to be shorter in G than in T H₂O₂.

The predicted trends have not yet been tested computationally in any systematic manner. However, it has been found that the N—H bond is elongated by 1.6% in NH₃²⁷ and the P—H bond by 3% in PH₃²⁸ as the molecules assume a nonplanar geometry.

The Effect of Ligand Electron Pairs — Beyond Monodeterminantal MO Theory

Fluorine is more electronegative than hydrogen and the 2*p* hydrogenic AO of fluorine is more electronegative than the 1*s* AO of hydrogen. This difference in 2*p_F* and 1*s_H* valence orbital electronegativities is responsible for stereochemical differences between H₂O and F₂O as well as between H₂O₂ and F₂O₂ for the reasons discussed in the previous sections. However, fluorine differs from hydrogen also in that it has three lone electron pairs while H has none. Since the bond diagrams of Figures 1 and 3 have been constructed by using only one valence AO per univalent ligand (2*p* for F and 1*s* for H), we still have to consider how our conclusions become modified once we recognize this second essential difference between F and H.

The bond diagrams for L and B F₂O, in which the F lone pairs are explicitly included, are shown in Figure 5. It is immediately evident that in addition to two core-ligand two-electron multicenter bonds there are now two core-ligand four-electron multicenter antibonds in linear as well as bent F₂O. As a result, the O—F bonds will become elongated so that the best compromise between core-ligand bonds and antibonds can be achieved. This means that in OF₂ core-ligand binding will be primarily due to the R CW itself with the core-ligand bonding due to the mixing of the R CW with other excited CW's becoming small. Let us refresh our memories as to why this is so.

Consider the two-electron bond of the simple diatomic A—A as described by VB theory. At the equilibrium bond distance, r_{eq} , the electronic wavefunctions, Ψ_e , is:

$$\Psi_e = A \cdot \cdot A + \lambda (A^+ + A^- + A^- \cdot A^+) \quad \lambda \ll 1$$

In this case, the bonding of A and A is due to spin pairing in the Heitler-London (HL) CW, $A \cdot \cdot A$, as well as to the mixing of $A \cdot \cdot A$ with $A^+ A^-$ and $A^- \cdot A^+$. When the A—A bond is appreciably »stretched«, the electronic wavefunction Ψ_s , becomes:

$$\Psi_s \approx A \cdot \cdot A$$

Now, the bonding of A and A is almost exclusively due to spin pairing in the HL CW mainly because the interaction of $A \cdot \cdot A$ with $A^+ A^-$, being primarily dependent on the AO resonance integral h_{12} which is a function of the AO

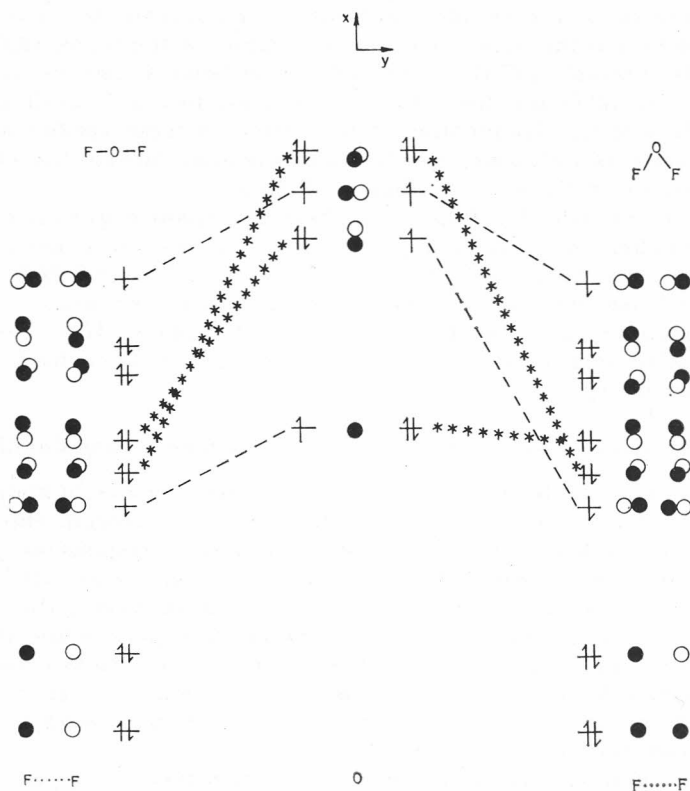


Figure 5. Principal compact MOVB diagrams for linear and bent OF_2 . Asterisks indicate four-electron antibonds.

overlap integral s_{12} , has been substantially weakened due to bond »stretching«. Finally, when r_{AA} becomes infinite, we obtain:

$$\Psi_d = A \cdot A$$

There is no longer any bonding of the atoms $A \cdot$ and $A \cdot$ due to spin pairing as the AO overlap integral is zero.

In MOVB theory, the role of the HL CW is played by the perfect pairing CW of lowest energy, denoted by R. When there is strong core-ligand binding, the correct ground state wavefunction is a linear combination of R and excited CW's and it can be represented by the appropriate bond diagram. When there is weak core-ligand binding, the ground state wavefunction can be approximated by the R CW. Finally, at the limit of infinite interfragmental distance, the R CW describes excited core and ligand fragments of maximum multiplicity in the absence of avoided diabatic surface crossing. In the case of interest, the R CW of OF_2 describes triplet O and triplet $F \cdots F$ when r_{O-F} becomes infinite. In short, the wavefunctions of strongly and weakly bound CL (C = core, L = ligands) systems are very different and this is expected to have stereochemical consequences reflecting the fact that in the former instance there is extensive delocalization while in the latter instance there is accentuated localization.

Monodeterminantal MO theory fails to describe correctly bond dissociation. At this level, the three (un-normalized) wavefunctions considered above are:

$$\Psi_e = A \cdot \cdot A + \lambda (A^+ A^- + A^- A^+) \quad \lambda = 1$$

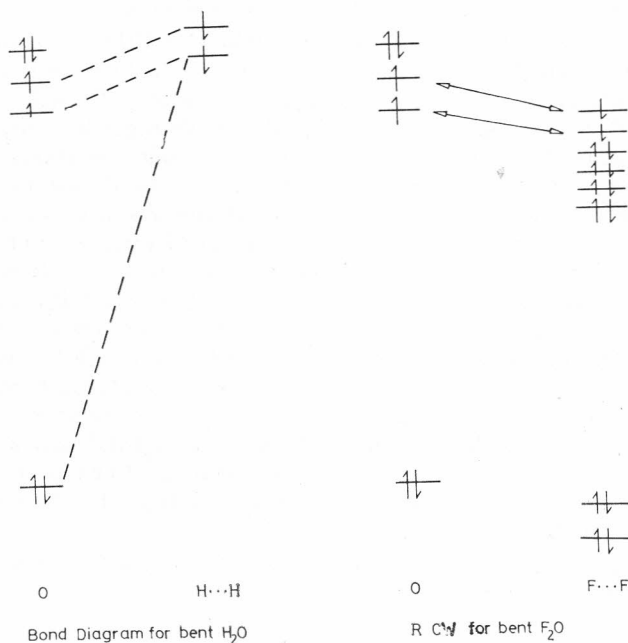
$$\Psi_s = A \cdot \cdot A + \lambda (A^+ A^- + A^- A^+) \quad \lambda = 1$$

$$\Psi_d = A \cdot \cdot A + \lambda (A^+ A^- + A^- A^+) \quad \lambda = 1$$

As can be seen, the CW compositions of all three wavefunctions are *identical*. It is now clear that the wavefunctions of equilibrium and »stretched« A—A are similar at the level of monodeterminantal MO theory. By analogy, the wavefunctions of strongly and weakly bound CL are similar and any difference in stereochemistry can only be due to differing *directionalities* of interfragmental charge transfer at the same level of theory.

The message of MOV B theory is loud and clear: F differs from H not only in terms of electronegativity but also in terms of overlap binding ability because the additional lone pairs enforce weak core-ligand bonding, whenever the core itself has a large number of lone pairs. This second difference cannot be perceived at the levels of HMO, EHMO, or SCF—MO theory simply because, at these levels of theory, bond dissociation is incorrectly described, *e. g.*, the total wavefunctions for equilibrium and »stretched« A—A have very similar CW compositions.

The above considerations suggest that the *difference* between H₂O and F₂O insofar as geometry is concerned are best reflected by *the detailed bond diagram* for bent H₂O and *the R CW* for bent F₂O, shown below.



[Double arrows indicate bonds]
due to spin pairing.]

The former implies that the O—H bonds are made by utilization of 2s and 2p oxygen AO's while the latter implies that the weak O—F bonds are indeed made by exclusive utilization of 2p oxygen AO's. Accordingly, this more complete analysis predicts that OF_2 will have a smaller angle than OH_2 , a conclusion which is identical to the one reached before by disregarding the effect of fluorine lone pairs and, hence, the consequences of weak core-ligand binding.

By using the same line of reasoning, we can show that the difference between H_2O_2 and F_2O_2 insofar as geometry is concerned is best reflected by *the bond diagram* of gauche H_2O_2 and *the R CW* of gauche F_2O_2 . Once again, this more complete analysis predicts that O_2F_2 will have a smaller dihedral angle than O_2H_2 , a conclusion which is identical to the one reached before by disregarding the effect of fluorine lone pairs. The situation is analogous to that encountered in the case of the H_2O and F_2O comparison. The above analysis implies the following: *The predictions of a smaller OF_2 bond angle (compared to H_2O) and a smaller O_2F_2 dihedral angle (compared to H_2O_2) by SD MO theory are qualitatively correct due to the fact that HMO, EHMO, and SCF—MO theory »see« part of the difference between H and F and this part is sufficiently compelling as to enforce the trend which is actually observed experimentally.*

Qualitative SD MO as well as qualitative MOVb theory both predict that B is more favorable than L OF_2 and that G is energetically preferable to T O_2F_2 , albeit for different reasons. Are there cases in which the two brands of theory give rise to different qualitative predictions? It is not difficult to identify two problems which further demonstrate that qualitative SD MO and qualitative MOVb theory are far from being close relatives. The first problem has to do with the O—O bond length in O_2X_2 and the second problem has to do with the absolute values of the dipole moments of OX_2 and O_2X_2 .

With respect to the O—O bond length, EHMO (= EHMOVb) theory predicts that $r_{\text{O-O}}$ in H_2O_2 will tend to $r_{\text{O-O}}$ in O_2^- and $r_{\text{O-O}}$ in F_2O_2 will tend to $r_{\text{O-O}}$ in O_2^+ . By contrast, MOVb theory predicts that $r_{\text{O-O}}$ in H_2O_2 will tend to r_{OO} in O_2^- but r_{OO} in F_2O_2 will tend to $r_{\text{O-O}}$ in O_2 . Also, with regards to dipole moments, monodeterminantal MO theory leads one to expect that the relative magnitudes of $\mu(\text{H}_2\text{O})$ and $\mu(\text{F}_2\text{O})$ as well as the relative magnitudes of $\mu(\text{H}_2\text{O}_2)$ and $\mu(\text{F}_2\text{O}_2)$ can be predicted from consideration of the absolute electronegativities of the constituent atoms and the classical concept of intrabond charge transfer. Since the atomic electronegativity difference between O and H is greater than that between O and F, it is predicted that $\mu(\text{OH}_2) > \mu(\text{OF}_2)$ and $\mu(\text{O}_2\text{H}_2) > \mu(\text{O}_2\text{F}_2)$. By contrast, while still predicting the same trends, MOVb theory suggests that the absolute magnitudes of $\mu_1(\text{F}_2\text{O})$ and $\mu(\text{F}_2\text{O}_2)$ will not be in keeping with expectations based on consideration of absolute atomic electronegativities and the classical concept of sigma »ionic« resonance simply because F_2O and F_2O_2 are weakly bound, they involve minimal delocalization, and they can be thought of as molecules made up of neutral atoms with bonds due to spin pairing. As a result, MOVb theory predicts that the dipole moments of F_2O and F_2O_2 will be »unexpectedly« small.

Experimental studies reveal that r_{OO} in F_2O_2 is nearly the same while r_{OO} in H_2O_2 is much larger than r_{OO} in O_2 .²⁹

Experimental dipole moment data for H₂O, F₂O, H₂O₂ and F₂O₂ are also available.³⁰

	H ₂ O	F ₂ O	H ₂ O ₂	F ₂ O ₂
μ /Debye:	1.85	0.29	2.26	1.44

However, in this case one cannot easily define what is »expected« and what is »unexpected« with regards to the absolute magnitudes of F₂O and F₂O₂. Hence, a more illuminating comparison must be sought. Indeed, the absolute dipole moments of NH₃ and NF₃ provide the ideal data for demonstrating the drawbacks of SD MO arguments. In this case, the atomic electronegativity difference between N and H and that between N and F are roughly the same. As a result, one would expect that the absolute dipole moments of NH₃ and NF₃ would be comparable. However, the fact is that NF₃ has a much smaller absolute dipole moment than NH₃.³¹

	NH ₃	NF ₃
μ /Debye:	1.47	0.24

Actually, this is a textbook example of the difficulties associated with the interpretation of dipole moments.³²

In closing, we mention some past contributions by other investigators which are related to this work. First, we remind the reader of the nice EHMO theoretical work of Hall⁶ who recognized the pivotal role of what we refer to as core excitation in determining the shape of H₂O. Secondly, we note that the momentous significance of the differential *s* and *p* overlap binding ability of atoms and how it varies along a column of the Periodic Table has been well recognized in an area of research which is not very familiar to most practicing organic chemists, namely, band theory of metals.³³ Thirdly, the profound implications of Δh [equation (7)] for molecular structure and, in particular, the differing structures of H₂O and H₂S have been recognized by Murrell, Kettle and Tedder who, in their excellent monograph entitled »Valence Theory«,³¹ give a VB rationalization of the smaller angle of H₂S as compared to H₂O which is largely equivalent to ours. Fourthly, we note a citation by Bauer and Yokozeki^{18e} which points out that the fact that the O—O bond length of F₂O₂ is very much like that of O₂ has been interpreted by Lipscomb to imply that F₂O₂ can be viewed as a triplet oxygen bound to two fluorines. Finally, we would like to mention the fact that an abundance of computations of H₂O, H₂O₂, and their derivatives does exist but space limitations do not allow us to demonstrate how they all can serve a useful purpose when interpreted through MOVb theory or its lower level approximate forms.

APPENDIX

Ethylene can be dissected into two CH₂ fragments, A and B, such that each contributes an *sp*² AO (denoted by *x*), a *2p* AO denoted by *y*), and two electrons towards carbon-carbon double bond formation. While ethylene has *D*_{2h} symmetry, each CH₂ fragment has local *C*_{2v} symmetry. Thus, the four AO's define two subsystems, one of *a*₁ and the other of *b*₁ symmetry as indicated below.

$$\begin{array}{c}
 \boxed{b_1 \quad y_1 - \quad - y_2 \quad b_1} = \Omega_1 (\Gamma_1 = a_1) \\
 \hline
 \boxed{a_1 \quad x_1 - \quad - x_2 \quad a_1} = \Omega_2 (\Gamma_2 = b_1) \\
 \hline
 \begin{array}{cc}
 \uparrow & \uparrow \\
 \text{Fragment} & \text{Fragment} \\
 \text{A} & \text{B}
 \end{array}
 \end{array}$$

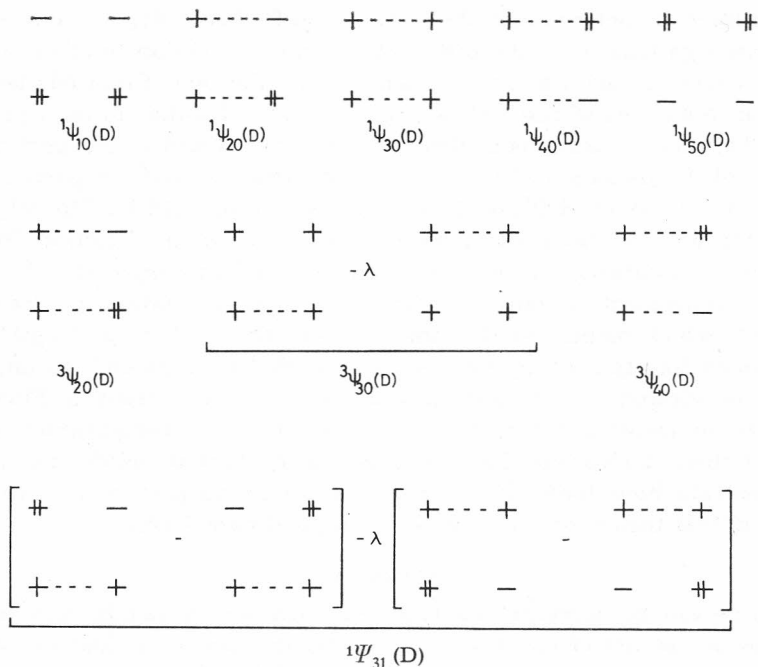
Starting with Ω_1 and Ω_2 and four electrons we generate the following MOVB Tableau's.

n_2	0	1	2	3	4
n_1	4	3	2	1	0
	T_1	T_2	T_3	T_4	T_5

The lower box corresponds to Ω_1 and the upper to Ω_2 with the former filled with n_1 and the latter n_2 electrons so that $n_1 + n_2 = 4$. Each T_i generates a U_i as follows:

$$T_1 \rightarrow U_1 (1) \quad T_2 \rightarrow U_2 (4) \quad T_3 \rightarrow U_3 (10) \quad T_4 \rightarrow U_4 (4) \quad T_5 \rightarrow U_5 (1)$$

The numbers in parenthesis indicate the number of CW's of each set. The singlet and triplet $\Psi_{i0}(D)$ are shown in Scheme 2.



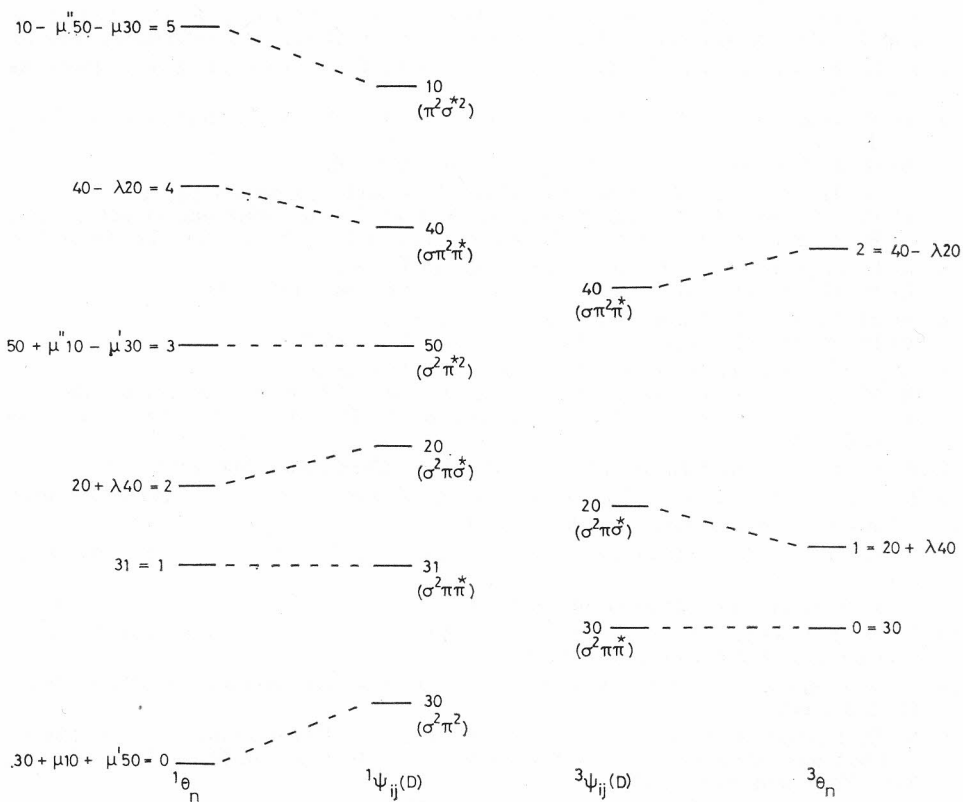
Scheme 2

The mathematical meaning of $\Psi_{i0}(D)$ is:

$$\psi_{10} = \begin{pmatrix} - & - \\ ++ & ++ \end{pmatrix}$$

$$\psi_{20} = c_1 \begin{pmatrix} + & - \\ + & ++ \end{pmatrix} + c_2 \begin{pmatrix} + & - \\ ++ & + \end{pmatrix} + c_3 \begin{pmatrix} - & + \\ ++ & + \end{pmatrix} + c_4 \begin{pmatrix} - & + \\ + & ++ \end{pmatrix}$$

Each parenthesis includes a single (spin adapted) CW. Singlet 30, 10, and 50 belong to the same irreducible representation and can mix. The same is true for singlet and triplet 20 and 40.

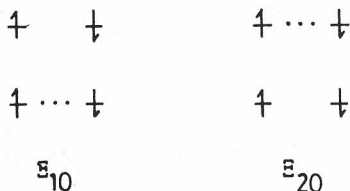


Scheme 3

According to the convention for choosing the partitions V_k^0 , none of $\Psi_{i0}(D)$ with $i = 2, 3, 4$ can be expressed as $\Psi_{i0}(R)$. However, we can always abandon this convention and express, e. g., ${}^1\Psi_{30}$ as follows:

$$\begin{aligned} {}^1\Psi_{30}(R) &\simeq c_{10} \mathcal{E}_{10} + c_{20} \mathcal{E}_{20} + \sum c_m \Phi_m \\ &\simeq c_{10} \mathcal{E}_{10} + c_{20} \mathcal{E}_{20} \end{aligned}$$

where $\bar{\epsilon}_{10}$ and $\bar{\epsilon}_{20}$ are:



The $\bar{\Phi}_m$'s are called extrinsic CW's. The analogy between MO and MOVb theory is projected in Scheme 3.

REFERENCES

1. For a recent spectroscopic study of H₂O see: R. L. Cook, F. C. Delucia, and P. Helminger, *J. Mol. Spectrosc.* **53** (1974) 62, and references therein.
2. R. L. Redington, W. B. Olson, and P. C. Cross, *J. Chem. Phys.* **36** (1962) 1311.
3. (a) *Molecular Geometry*, R. J. Gillespie, Van Nostrand Reinhold Co.: London, 1972.
(b) R. J. Gillespie, *J. Chem. Educ.* **51** (1974) 367.
4. (a) A. D. Walsh, *J. Chem. Soc.* (1953) 2260 and subsequent papers.
(b) For review of the Mulliken-Walsh MO model of molecular structure see: R. J. Buenker and S. D. Peyerimhoff, *Chem. Rev.* **74** (1974) 127.
5. (a) L. S. Bartell, *J. Chem. Educ.* **45** (1968) 754.
(b) R. G. Pearson, *J. Amer. Chem. Soc.* **91** (1969) 1252, 4947.
6. (a) M. B. Hall, *Inorg. Chem.* **17** (1978) 2261.
(b) M. B. Hall, *J. Amer. Chem. Soc.* **100** (1978) 6333.
7. (a) C. C. Levin, *J. Amer. Chem. Soc.* **97** (1975) 5649.
(b) W. Cherry and N. D. Epiotis, *J. Amer. Chem. Soc.* **98** (1975) 1135.
(c) W. Cherry, N. D. Epiotis, and W. T. Borden, *Acc. Chem. Res.* **10** (1977) 167.
8. W. E. Palke and B. Kirtman, *J. Amer. Chem. Soc.* **100** (1978) 5717.
9. E. Shustorovich and P. A. Dobosh, *J. Amer. Chem. Soc.* **101** (1979) 4090.
10. S. Wolfe, *Acc. Chem. Res.* **5** (1972) 102.
11. L. Radom, W. J. Hehre, and J. A. Pople, *J. Amer. Chem. Soc.* **94** (1972) 2371.
12. J. A. Pople, *Tetrahedron* **30** (1974) 1605.
13. N. D. Epiotis, W. R. Cherry, S. Shaik, R. L. Yates, and F. Bernardi, *Top. Curr. Chem.* **70** (1977) 1.
14. G. Winnewisser, M. Winnewisser, and W. Gordy, *J. Chem. Phys.* **47** (1968) 3465.
15. N. D. Epiotis, J. R. Larson, and H. Eaton, *Unified Valence Bond Theory of Electronic Structure*, in: *Lecture Notes in Chemistry*, Vol. 29, Springer-Verlag: New York and Berlin, 1982.
16. N. D. Epiotis, *Unified Valence Bond Theory of Electronic Structure. Applications*, in: *Lecture Notes in Chemistry*, Vol. 34; Springer-Verlag: New York and Berlin, 1983.
17. A. W. Potts, and W. C. Price, *Proc. R. Soc. London, Ser. A* (1972) 326, 165.
18. (a) J. H. Lambert, *Pyramidal Atomic Inversion*, in: *Topics in Stereochem.* **6** (1966) 19.
(b) A. Rauk, L. C. Allen, and K. Mislow, *Angew. Chem. Int. Ed. Engl.* **9** (1970) 400.
(c) K. Mislow, *Trans. N. Y. Acad. Sci.* **35** (1973) 227.
(d) R. J. Buenker and S. D. Peyerimhoff, *Chem. Rev.* **74** (1974) 127.
(e) A. Yokozeki and S. H. Bauer, *Top. in Curr. Chem.* **53** (1974) 71.

19. (a) OF₂: L. Pierce, R. Jackson, and N. DiCianni, *J. Chem. Phys.* **35** (1961) 2240.
 (b) OH₂: Ref. 1.
 (c) O(CH₃)₂: K. Kimura and M. Kubo, *J. Chem. Phys.* **30** (1959) 151.
 (d) O(SiH₃)₂: A. Almennigen, O. Bastiansen, V. Ewing, K. Hedberg, and M. Traetteberg, *Acta Chem. Scand.* **17** (1963) 2455.
20. (a) NF₃: M. Ootake, C. Matsumura, and Y. Morino, *J. Mol. Spectrosc.* **28** (1968) 325.
 (b) NH₃: M. T. Weiss and M. W. P. Strandbert, *Phys. Rev.* **83** (1951) 567.
 (c) N(CH₃)₃: B. Beagley and T. G. Hewitt, *Trans. Faraday Soc.* **64** (1968) 2651.
 (d) N(SiH₃)₃: G. Beagley and A. R. Conrad, *ibid.* **66** (1970) 2740.
21. C. A. Burrus and W. Gordy, *Phys. Rev.* **92** (1953) 274.
22. M. Wolfsberg and L. Helmholz, *J. Chem. Phys.* **20** (1952) 387.
23. See Table I of Ref. 13.
24. The differing magnitudes of Δh_X are responsible for the fact that H₂X = XH₂, where X = C, Si, Ge, Sn, adopt different geometries with H₂C = CH₂ being planar but H₂Sn = SnH₂ being trans-bent (see ref. 16, Chapter 21).
25. For a detailed discussion of the relative overlap binding abilities of different atoms in a fixed hybridization state and the attendant stereochemical consequences, see ref. 16 and especially Chapters 1 and 2.
26. Up to this point the same conclusions can be obtained if MOVb is replaced by EHMovH (=EHMO) theory. At this level, the analysis can be based on the Independent Bond Model,^{15,16} according to which a given species can be viewed as a product of subsystem wavefunctions, Ω_i (see Scheme 1), with its total energy being a simple sum of subsystem energies since »classical« coulomb interaction is neglected.
27. L. C. Allen, E. Clementi, and A. Rauk, *J. Chem. Phys.* **52** (1970) 4133.
28. J. M. Lehn and B. Munsch, *Mol. Phys.* **23** (1971) 91.
29. (a) O₂F₂: R. H. Jackson, *J. Chem. Soc.* (1962) 4585.
 (b) O₂: *Spectra of Diatomic Molecules*, G. Herzberg, Van Nostrand, Princeton, 1950.
 (c) O₂H₂: R. L. Redington, W. B. Olson, and P. C. Cross, *J. Chem. Phys.* **36** (1962) 1311.
 (d) O₂⁻: R. F. W. Bader, W. H. Henneker, and P. E. Cade, *J. Chem. Phys.* **46** (1967) 3341.
30. (a) H₂O: G. Birnbaum and S. K. Chatterjie, *J. Appl. Phys.* **23** (1952) 220.
 (b) F₂O, H₂O₂, F₂O₂: *Dipole Moments in Inorganic Chemistry*, G. J. Moody, and J. D. R. Thomas, Edward Arnold, London, 1970.
31. (a) NH₃: D. K. Coles, W. E. Good, J. K. Bragg, and A. H. Sharbaugh, *Phys. Rev.* **82** (1951) 877.
 (b) NF₃: P. Kisliuk, *J. Chem. Phys.* **22** (1954) 86.
32. *Organic Chemistry*, 2nd Ed. T. W. G. Solomons, John Wiley and Sons: New York, 1980, p. 19.
33. *Solid State Quantum Chemistry*, A. A. Levin, McGraw-Hill: New York, 1977.
34. *Valence Theory*, 2nd Ed., J. N. Murrell, S. F. A. Kettle, and J. M. Tedder, John Wiley and Sons: New York, 1970.

SAŽETAK

Metoda »zajedničkih nazivnika« s pomoću MOVb pristupa: struktura molekula H₂O, H₂O₂ i njihovih derivata

Nicolaos D. Epiotis, James R. Larson i Hugh H. Eaton

Detaljno je ilustrirana primjena kvalitativne MOVb-teorije na probleme stereokemije molekula H₂O, H₂O₂ i njihovih derivata. Pri tome su dani rezultati teorijskih pristupa različitim stupnjevā složenosti. Pokazano je da je problem geometrija sustava H₂O i H₂O₂ u svojoj biti (tj. u prvoj aproksimaciji) isti.